http://dx.doi.org/10.11142/jicems.2013.2.1.23
Journal of International Conference on Electrical Machines and Systems Vol. 2, No. 1, pp.23 ~30 , 2013 23

Winding Turn-to-Turn Faults Detection of Fault-Tolerant Permanent-Magnet Machines Based on a New Parametric Model

Guohai Liu *, Wei Tang * and Wenxiang Zhao *

Abstract –This paper proposes a parametric model for inter-turn fault detection in a fault-tolerant permanent-magnet (FTPM) machine, which can predict the effect of the short-circuit fault to various physical quantity of the machine. For different faulty operations, a new effective stator inter-turn fault detection method is proposed. Finally, simulations of vector-controlled FTPM machine drives are given to verify the feasibility of the proposed method, showing that even single-coil short-circuit fault could be exactly detected.

Keywords: Fault-tolerant permanent-magnet machine, Fault detection, Short-circuit, Current harmonic

1. Introduction

Due to high efficiency, high power density and high reliability, fault-tolerant permanent-magnet (FTPM) machines have been widely studied for many applications such as aerospace and electric vehicle (EV) [1]-[3]. The major faults of the FTPM machines can be classified as air-gap eccentricity, bearing failures, demagnetized magnet and stator wingding faults (open-circuit and short-circuit faults). Inter-turn short-circuit fault is one of the most common fault types which are usually related to insulation degradation and could develop into more serious results [4]. Also, it is one of the most different failures to diagnose, especially when single-turn short circuit occurs.

Many effective techniques have been presented to detect inter-turn short-circuit fault in the past years, and majority of them focused on induction machines [5]. Recently, some effective diagnostic methods for PM machines have been proposed such as electromagnetic torque waveform and the summation of phase voltages [6], reference voltages [7], high-frequency (HF) injection [8]. In [9], the change of the flux was used to identify the short-circuit fault, but an extra search coil should be placed in the stator teeth for this fault detection. The model of self-inductance and mutual-inductance was investigated in [10], however, the resistance of the shorted part was not considered. Very recently, a new five-phase FTPM machines were proposed for four-wheel independently driven EVs as shown in Fig. 1 [11], offering high fault-tolerant capability. Although there is a number of PM machine model with inter-turn fault [12], [13], the model of five-phase fault-tolerant machine with stator inter-turn fault is unavailable.

In this paper, a new dynamic model of the five-phase FTPM machine under short-circuit fault will be developed. The mathematical equations are derived in detail. Finally, simulated results are given for the faulty machine to verify the proposed inter-turn short-circuit fault detection method.

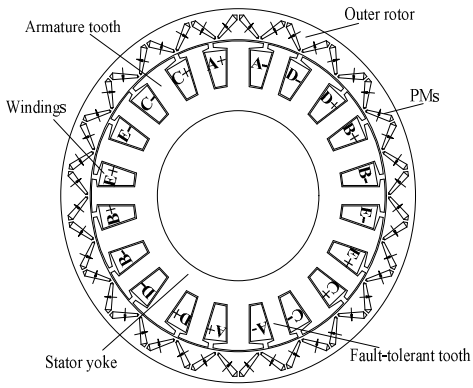

Fig. 1. Cross-section of five-phase FTPM machine.

2. Stationary and Rotating Frame Models

In this section, the five-phase FTPM machine models under healthy and inter-turn short-circuit fault conditions will be derived in stationary and rotating frames, respectively. The following assumptions are made.

1) The unbalance of machine itself is neglected.
2) The magnetic saturation is ignored.
3) The permeability of iron is infinite.
4) The symmetry condition is ideal.

* School of Electrical and Information Engineering, Jiangsu University, China. (ghliu@ujs.edu.cn; tweiabc@163.com; zwx@ujs.edu.cn)
Received 23 December 2012; Accepted 31 January 2013

2.1 Healthy Machine in Stationary Frame

The stator equation for a healthy five-phase FTPM machine in stationary frames is given as:

$$[V_{sh}]=[R_{sh}][i_{sh}]+\frac{d}{dt}[\psi_{sh}] \tag{1}$$

The stator magnetic flux is:

$$[\psi_{sh}]=[L_{sh}][i_{sh}]+[\psi_{PM}] \tag{2}$$

where Ψ_{PM} is the PM flux linkage.

From (1) and (2), the general equation is calculated as:

$$[V_{sh}]=[R_{sh}][i_{sh}]+[L_{sh}]\frac{d}{dt}[i_{sh}]+[e_h] \tag{3}$$

where $[V_{sh}]=[V_a\ V_b\ V_c\ V_d\ V_e]^T$, $[i_{sh}]=[i_a\ i_b\ i_c\ i_d\ i_e]^T$,

$$[R_{sh}]=\begin{bmatrix} R_s & 0 & 0 & 0 & 0\\ 0 & R_s & 0 & 0 & 0\\ 0 & 0 & R_s & 0 & 0\\ 0 & 0 & 0 & R_s & 0\\ 0 & 0 & 0 & 0 & R_s \end{bmatrix},[L_{sh}]=\begin{bmatrix} L & M_0 & M_1 & M_1 & M_0\\ M_0 & L & M_0 & M_1 & M_1\\ M_1 & M_0 & L & M_0 & M_1\\ M_1 & M_1 & M_0 & L & M_0\\ M_0 & M_1 & M_1 & M_0 & L \end{bmatrix}$$

and $[e_h]=[E_a\ E_b\ E_c\ E_d\ E_e]^T$, in which R_s is the stator resistance, L, M_0 and M_1 are the phase self-inductance and mutual-inductance, the subscript, '0' and '1', represent the adjacent phase and nonadjacent phase, respectively. However, the machine used for fault-tolerant applications has a minimized mutual-inductance. The structure of the machine has been designed as shown in Fig. 1, and its fault-tolerant teeth could reduce the mutual-inductance. Hence, their relations are given as $M_0=M_1=M=0$.

The electromagnetic torque equation in stationary frame is given as

$$T_e=\frac{E_a i_a+E_b i_b+E_c i_c+E_d i_d+E_e i_e}{\Omega} \tag{4}$$

where Ω is the mechanical angular speed and E_i is back-EMF of phase-i.

2.2 Healthy Machine in Rotating Frame

The Concordia/Clarke and Park transforms used to convert magnitudes from stationary frame to rotating frame have been successfully applied to the existing machine control schemes. It could be extended to multi-phase FTPM machines and the reference frame theory from n-phase to two-phase is given in [14].

Fig. 2 shows the coordinate transformation diagram. The transformation equation of convert variables from the stationary reference to the synchronously-rotating frame can be expressed as:

$$[X_{dq}]=T(\theta)[X_{abcde}] \tag{5}$$

where $T(\theta)$ is the Extended Park transformation matrix, which is given as:

$$T(\theta)=\frac{2}{5}\begin{bmatrix} \cos\theta & \cos(\theta-\frac{2\pi}{5}) & \cos(\theta-\frac{4\pi}{5}) & \cos(\theta-\frac{4\pi}{5}) & \cos(\theta-\frac{2\pi}{5})\\ -\sin\theta & -\sin(\theta-\frac{2\pi}{5}) & -\sin(\theta-\frac{4\pi}{5}) & -\sin(\theta-\frac{4\pi}{5}) & -\sin(\theta-\frac{2\pi}{5})\\ 1 & \cos\frac{2\pi}{5} & \cos\frac{4\pi}{5} & \cos\frac{4\pi}{5} & \cos\frac{2\pi}{5}\\ 0 & \sin\frac{2\pi}{5} & \sin\frac{4\pi}{5} & -\sin\frac{4\pi}{5} & -\sin\frac{2\pi}{5}\\ \frac{1}{\sqrt{2}} & \frac{1}{\sqrt{2}} & \frac{1}{\sqrt{2}} & \frac{1}{\sqrt{2}} & \frac{1}{\sqrt{2}} \end{bmatrix} \tag{6}$$

where θ is the rotor electrical position.

By applying the Extended Park transformation matrix to the equations in stationary, the stator equations can be written as:

$$V_{dh}=R_s i_d-w(L-M)i_q+(L-M)\frac{di_d}{dt} \tag{7}$$

$$V_{qh}=R_s i_q+w(L-M)i_d-(L-M)\frac{di_q}{dt}+w\psi_{PM} \tag{8}$$

The electromagnetic torque equation is expressed as:

$$T_e=\frac{5}{2}p[i_q\psi_{PM}+(L_d-L_q)i_d i_q] \tag{9}$$

where p is the number of the pole pairs.

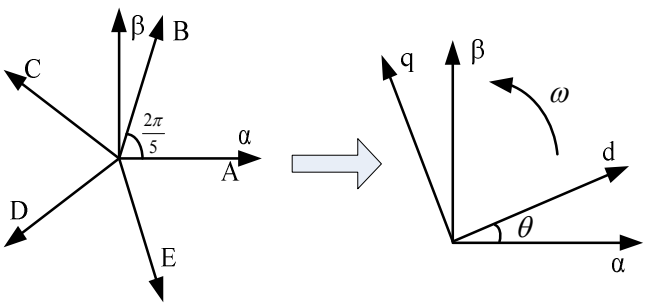

Fig. 2. Coordinate transformation from stationary frame to d-q frame.

The effect of saliency on the rotor yields could be neglected in the Interior PM machine, the electromagnetic torque equation can now be evaluated as:

$$T_e = \frac{5}{2} p i_q \psi_{PM} \tag{10}$$

The mechanical equation is as follows:

$$T_e = J\frac{d\omega}{dt} + B\omega + T_L \tag{11}$$

where B is the frictional coefficient and J is the moment of inertia.

2.3 Faulty Machine in Stationary Frame

An inter-turn fault is usually related to insulation failures between two adjacent windings. Fig. 3 shows a five-phase FTPM machine with inter-turn fault in phase a, in which a_1 and a_2 represent the healthy turns and the faulted turns, respectively, r_f is used to simulate the fault insulation resistance.

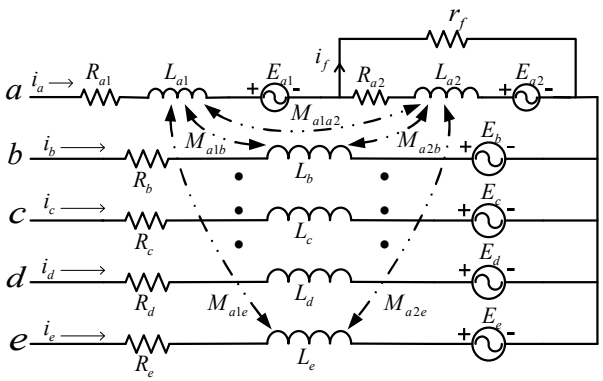

Fig. 3. Diagram of the five-phase fault-tolerant PMSM with stator inter-turn faults in phase a.

The relations of the parameters in the fault phase are expressed as:

$$\begin{cases} R_{a1} + R_{a2} = R_a \\ E_{a1} + E_{a2} = E_a \\ L_{a1} + L_{a2} + 2M_{a1a2} = L_a \end{cases} \tag{12}$$

The stator equation for five-phase fault-tolerant FTPM machine with inter-turn fault in stationary frame is given as:

$$\left[V_{sf}\right] = \left[R_{sf}\right]\left[i_{sf}\right] + \left[L_{sf}\right]\frac{d}{dt}\left[i_{sf}\right] + \left[e_f\right] \tag{13}$$

From the short-circuit loop in the Fig. 3, the equations could be obtained as:

$$\begin{cases} V_{a1} + V_{a2} = V_a \\ V_{a2} = r_f i_f \\ E_{a2} = E_f \end{cases} \tag{14}$$

It is assumed that μ is the ratio of fault turns n out of the total turns N in phase a, resulting in $\mu = n/N$.

Then the faulty resistance R_{a2} and inductance which related to the fault wingding can be expressed as follows:

$$\begin{cases} R_{a2} = \mu R_s \\ L_{a2} = \mu^2 L \\ M_{a1a2} = \mu(1-\mu)L \end{cases} \tag{15}$$

$$M_{a1b} = M_{a1c} = M_{a1d} = M_{a1e} = \mu M \tag{16}$$

Based on (12)-(16), the parameters of the FTPM machine can be derived as:

$$\left[V_{sf}\right] = \left[V_a \;\; V_b \;\; V_c \;\; V_d \;\; V_e \;\; 0\right]^T \tag{17}$$

$$\left[i_{sf}\right] = \left[i_a \;\; i_b \;\; i_c \;\; i_d \;\; i_e \;\; i_f\right]^T \tag{18}$$

$$\left[R_{sf}\right] = \begin{bmatrix} R_s & 0 & 0 & 0 & 0 & -\mu R \\ 0 & R_s & 0 & 0 & 0 & 0 \\ 0 & 0 & R_s & 0 & 0 & 0 \\ 0 & 0 & 0 & R_s & 0 & 0 \\ 0 & 0 & 0 & 0 & R_s & 0 \\ -\mu R & 0 & 0 & 0 & 0 & \mu R + r_f \end{bmatrix} \tag{19}$$

$$\left[L_{sf}\right] = \begin{bmatrix} L & M & M & M & M & -\mu L \\ M & L & M & M & M & -\mu M \\ M & M & L & M & M & -\mu M \\ M & M & M & L & M & -\mu M \\ M & M & M & M & L & -\mu M \\ -\mu L & -\mu M & -\mu M & -\mu M & -\mu M & \mu^2 L \end{bmatrix} \tag{20}$$

The electromagnetic torque equation with intern-turn fault in stationary frame can be expressed as:

$$T_{ef} = \frac{E_a i_a + E_b i_b + E_c i_c + E_d i_d + E_e i_e - E_f i_f}{\Omega} \tag{21}$$

2.4 Faulty Machine in Rotating Frame

When the FTPM machine is with the inter-turn fault, the fault current circulates in the short circuit loop only. Hence, the Extended Park transformation in fault condition will change as:

$$T(\theta)=\frac{2}{5}\begin{bmatrix} \cos(\theta) & \cos(\theta-\frac{2\pi}{5}) & \cos(\theta-\frac{4\pi}{5}) & \cos(\theta+\frac{4\pi}{5}) & \cos(\theta+\frac{2\pi}{5}) & 0 \\ -\sin(\theta) & -\sin(\theta-\frac{2\pi}{5}) & -\sin(\theta-\frac{4\pi}{5}) & -\sin(\theta+\frac{4\pi}{5}) & -\sin(\theta+\frac{2\pi}{5}) & 0 \\ 1 & \cos\frac{2\pi}{5} & \cos\frac{4\pi}{5} & \cos\frac{4\pi}{5} & \cos\frac{2\pi}{5} & 0 \\ 0 & \sin\frac{2\pi}{5} & \sin\frac{4\pi}{5} & -\sin\frac{4\pi}{5} & -\sin\frac{2\pi}{5} & 0 \\ \frac{1}{\sqrt{2}} & \frac{1}{\sqrt{2}} & \frac{1}{\sqrt{2}} & \frac{1}{\sqrt{2}} & \frac{1}{\sqrt{2}} & 0 \\ 0 & 0 & 0 & 0 & 0 & \frac{5}{2} \end{bmatrix} \quad (22)$$

By applying the Extended Park transformation matrix to the stator equation (13), the result will be obtained as:

$$\begin{aligned} \left[V_{dq\_f}\right] &= T(\theta)\cdot[R_f]\cdot T^{-1}(\theta)\cdot[i_{dq\_f}] \\ &+T(\theta)\cdot[L_f]\cdot\frac{dT^{-1}(\theta)}{dt}\cdot[i_{dq\_f}]+T(\theta)\cdot[L_f]\cdot T^{-1}(\theta)\cdot\frac{d[i_{dq\_f}]}{dt} \\ &+T(\theta)\cdot\frac{dT^{-1}(\theta)}{dt}\cdot[\Psi_{PMf\_dq}]+T(\theta)\cdot T^{-1}(\theta)\cdot\frac{d[\Psi_{PMf\_dq}]}{dt} \end{aligned} \quad (23)$$

where $\left[V_{dq\_f}\right]=\left[V_d\ V_q\ V_0\ 0\right]^T$, $\left[i_{dq\_f}\right]=\left[i_d\ i_q\ i_0\ i_f\right]^T$.

Then, the stator equations for the five-phase FTPM machine in rotating frame are expressed as:

$$\begin{aligned} V_d &= R_s i_d - w(L-M)i_q - \frac{2}{5}\mu R_s i_f\cos\theta \\ &+(L-M)\frac{di_d}{dt}-\frac{2}{5}\mu(L-M)\cos\theta\frac{di_f}{dt} \end{aligned} \quad (24)$$

$$\begin{aligned} V_q &= R_s i_q + w(L-M)i_d + \frac{2}{5}\mu R_s i_f\sin\theta \\ &+(L-M)\frac{di_q}{dt}+\frac{2}{5}\mu(L-M)\cos\theta\frac{di_f}{dt}+w\Psi_{PM} \end{aligned} \quad (25)$$

Also, the equation in the shorted turns is written:

$$\begin{aligned} 0 &= \mu\left[w(L-M)\sin\theta-R_s\cos\theta\right]i_d+(\mu R_s+r_f)i_f \\ &-\mu(L-M)\cos\theta\frac{di_d}{dt}+\mu\left[w(L-M)\cos\theta+R_s\sin\theta\right]i_q \\ &+\mu(L-M)\sin\theta\frac{di_q}{dt}+\mu^2L\frac{di_f}{dt}+\mu w\Psi_{PM}\sin\theta \end{aligned} \quad (26)$$

The electromagnetic torque is given as:

$$T_{ef}=\frac{\partial W_{co}}{\partial\theta} \quad (27)$$

where W_{co} is the co-energy and is defined as:

$$W_{co}=\frac{1}{2}\left[i_{sf}\right]^T\left[L_{sf}\right]\left[i_{sf}\right]+\left[i_{sf}\right]^T\left[\psi_{PMf}\right] \quad (28)$$

Considering that there is no saliency on the rotor yields, the torque equation can be derived as:

$$T_{ef}=P\left[i_{sf}\right]^T\frac{\partial\left[\Psi_{PM}\right]}{\partial\theta} \quad (29)$$

Additionally, i_{sf} can be expressed as:

$$i_{sf}=T(\theta)^{-1}\left[i_{dq\_f}\right] \quad (30)$$

Substituting (30) into (29)

$$T_{ef}=\frac{5}{2}P\left[\Psi_{PM}\right]i_q-\mu P\left[\Psi_{PM}\right]i_f\sin\theta \quad (31)$$

The mechanical equation is as follows:

$$T_{ef}=J\frac{d\omega}{dt}+B\omega+T_L \quad (32)$$

3. Verification

The machine is upon the operation of vector-controlled PMSM drives as shown in Fig. 4. The FTPM machine is fed by a five-leg voltage source inverter (VSI), the system contains an outer speed-regulating loop and an inner current-regulating loop.

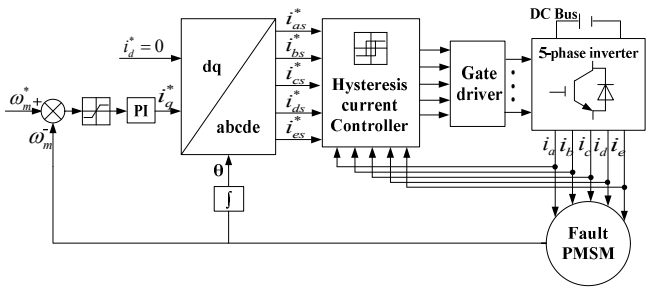

Fig. 4. Block diagram of the vector control PMSM drives system.

Table 1 shows the machine specifications. The stator

winding consists of 27 turns of each phase and the machine operates at 1500 r/min, a load torque of 6 Nm was applied to the motor at 0.02s under the shorted turn of 1/27 (3.7%), 2/27 (7.4%) and 3/27 (11.1%), respectively.

Table1. Specification of the Five-Phase Fault-Tolerant Permanent-Magnet Machine.

Speed	1500 r/min	Phase resistance	0.048 Ω
Torque	6 Nm	Phase inductance	3.1 mH
Back EMF (peak)	60 V	Number of phase	5
DC supply voltage	200 V	Number of pole-pairs	11
PM flux linkage	0.034 Wb	Turns per phase winding	27

Fig. 5 shows the simulated results of the fault current i_f. As the number of shorted turns increase, it can be seen that the magnitude of i_f becomes smaller, since the short fault will change the parameters of the machine and form a short circuit loop. In fact, due to the effect of the short fault, the inducted voltage and impedance are related to the number of turns. Moreover, the induced voltage and the resistance are in proportion to the number of turns. However, the reactance is proportional to the square of the number of the turns. As the fault extends, the change of impedance is faster than that of the induce voltage. Therefore, the amplitude of the fault current becomes smaller.

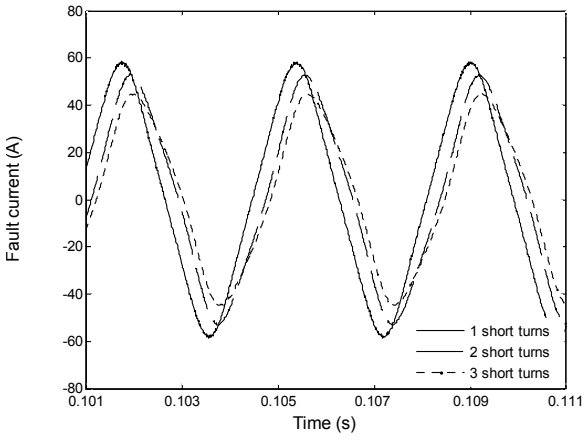

Fig. 5. Shorted circuit current i_f for different fault levels.

Fig. 6 shows the simulated results of q-axis current obtained from the proposed model. It can be seen from Fig. 6(a) that the inter-turn fault generates ripple in i_q current. Also, the ripple becomes severe as the failure extends. This is because when the fault occurred, the machine would operate in an unbalance condition. As a result, the unbalance effect generates second harmonic components in q-axis current, resulting in the oscillation. However, the root-mean-square (RMS) of the q-axis current becomes smaller as shown in Fig. 6(b). The actual speed of the machine is regulated to set value by the speed-regulating loop, although there is a little ripple (see Fig. 7). When the fault occurs, the magnitude is small enough to be negligible. Then, it can be deduced that $dw/dt \approx 0$. Also, by considering the Equ. (31), the Equ. (32) can be rewritten as:

$$\frac{5}{2}P\left[\Psi_{PM}\right]i_q - \mu P\left[\Psi_{PM}\right]i_f \sin\theta - B\omega - T_L = 0 \qquad (33)$$

When T_L is given, the current i_q is mainly determined by the fault current i_f. As stated previously, fault current i_f decreases with the fault expanding, resulting in the reduction of the RMS of i_q.

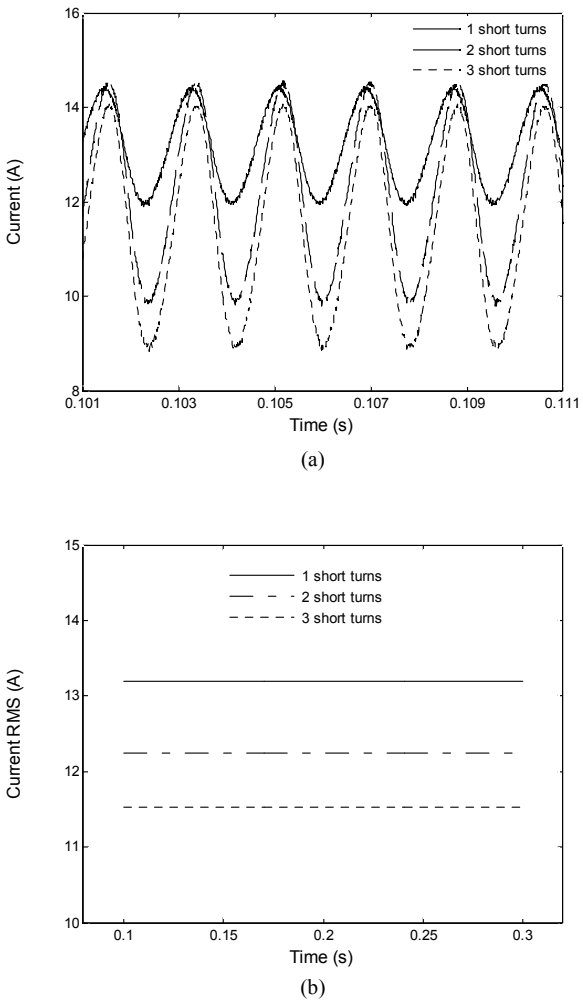

Fig. 6. Simulated result of q-axis current for different shorted circuit number. (a) Current waveforms of i_q. (b) RMS of q-axis current

Fig.8 shows the simulated electromagnetic torque waveforms under single-turn shorted condition. It can be seen that the electromagnetic torque is oscillatory in faulty condition. By comparing the electromagnetic torque Equ. (10) and (31), it can be seen that there is a braking torque component developed by the fault current when shorted fault occurs. Obviously, the direction of the fault current circulated around the shorted loop is opposite to that of the phase current flowed in healthy windings, as shown in Fig. 3. Then the interaction between the EMF and short current emerged in the shorted loop generates a breaking torque component, which causes pulse in the electromagnetic torque.

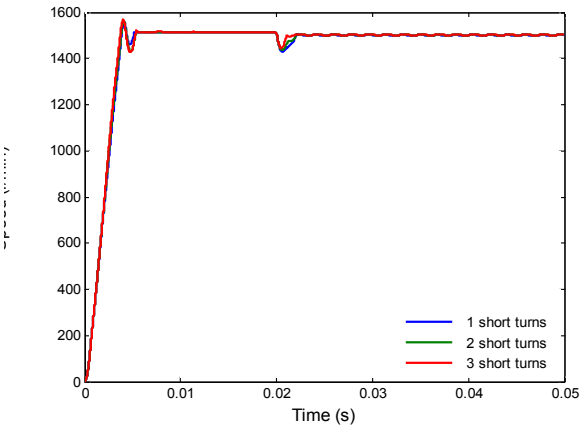

Fig.7. Simulated result of speed with intern-turn short fault.

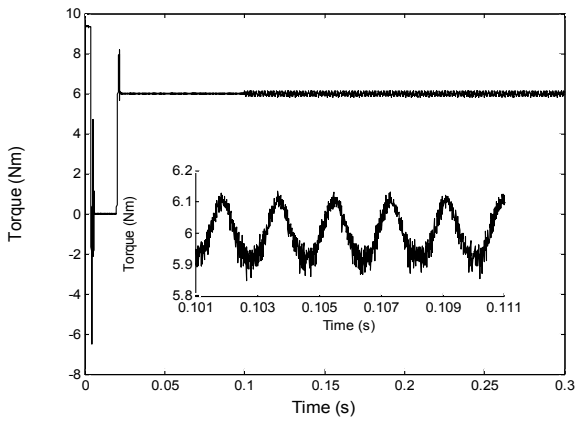

Fig. 8. Simulated result of torque for single-coil short-circuit fault.

As previously discussed, although the amplitude of the different signals depends on the inter-turn fault severity, these signals are usually affected by the given angular speed such as load torque. Therefore, they cannot be used to indicate the fault severity. However, the second-order harmonic components in the *q*-axis current mainly affected by the fault severity, in other words, it could neglect the effect created by the variation of the given. So, the second-order harmonic components of the *q*-axis current can be chosen as the fault indicator used to reveal fault and its severity. Further observation from Fig. 9 reveals that the second harmonic components content in *q*-axis current with different number of turns shorted under a certain given 1500 r/min and 6 Nm. It can be known that as the number of turns in short circuit increase, the content of second harmonic in *q*-axis current also augments.

Table 2 shows the variation of the second-order harmonic content of *q*-axis current when the machine operates under fault conditions with different given. It could be seen that, although the second harmonic content will change with the variation of the given, the magnitude of the variation is in a smaller range under the certain fault level. However, the second harmonic changes most significantly with the fault extending, and the range of the change has little relation to the variation of the given.

From the above analysis, it can be concluded that the second harmonic content used to indicate the fault could reveal the short-turn fault severity exactly and almost not affected by the variation of the given.

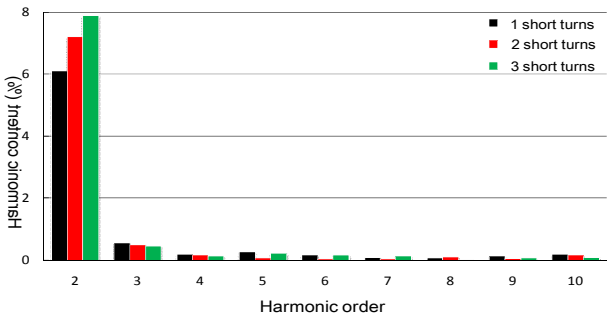

Fig. 9. Simulated result of the harmonic analysis for *q*-axis current.

Table2. Second harmonic content of Q-axis current with different given of speed and torque

Torque (NM)	Fault Severity	Second Harmonic Content(%)		
		500 (R/min.)	1000 (R/min.)	1500 (R/min.)
3	1 Short turns	5.982	6.032	5.974
	2 Short turns	7.297	7.325	7.311
	3 Short turns	7.952	8.032	7.960
6	1 Short turns	6.013	5.915	6.109
	2 Short turns	7.132	7.342	7.213
	3 Short turns	7.888	7.914	7.885

4. Conclusion

A new parametric model of five-phase FTPM machine have been developed, and the model could reflect the mechanism of the effect caused by inter-turn fault to the performance characteristics of the machine, which can be used as a basis for fault diagnosis and condition monitoring.

Simulated results have verified that the model is effective and detailed analysis has been given to illustrate the effect of inter-turn fault to machines operating performance. The second-order harmonic of *q*-axis has been used to indicate the fault, the proposed fault diagnosis approach is simple and no extra sensor is required, which also could realize on-line detection.

Acknowledgements

This work was supported in part by the National Natural Science Foundation of China (Projects 51077066, 61273154 and 51277194), by the Specialized Research Fund for the Doctoral Program of Higher Education of China (Project 20123227110012), by the Natural Science Foundation of Jiangsu Province (Project BK2012711), by the Fund Program of Jiangsu University for Excellent Youth Teachers and by the Priority Academic Program Development of Jiangsu Higher Education Institutions.

References

[1] W. Cao, B. C. Mecrow, G. J. Atkinson, J. W. Bennett, and D. J. Atkinson, "Overview of Electric Motor Technologies Used for More Electric Aircraft (MEA)," *IEEE Trans. Ind. Electron.*, vol. 59, no. 9, pp. 3523-3531, Sep. 2012.

[2] R. Cao, C. Mi, and M. Cheng, "Quantitative Comparison of Flux-Switching Permanent-Magnet Motors with Interior Permanent Magnet Motor for EV, HEV, and PHEV applications," *IEEE Trans. Magn.*, vol. 48, no. 8, pp. 2374-2384, Aug. 2012.

[3] W. Zhao, M. Cheng, K. T. Chau, J. Ji, and R. Cao, "Remedial Injected Harmonic Current Operation of Redundant Flux-Switching Permanent Magnet Motor Drives," *IEEE Trans. Ind. Electron.*, vol. 60, no. 1, pp. 151-159, Jan. 2013.

[4] A. Gandhi, T. Corrigan, and L. Parsa, "Recent Advances in Modeling and Online Detection of Stator Interturn Faults in Electrical Motors," *IEEE Trans. Ind. Electron.*, vol. 58, no. 5, pp. 1564-1575, May. 2011.

[5] A. Bellini, F. Filippetti, C. Tassoni, and G. A. Capolino, "Advances in Diagnostic Techniques for Induction Machines," *IEEE Trans. Ind. Electron*., vol. 55, no. 12, pp. 109-4126, Dec. 2008.

[6] M. A. Awadallah, M. M. Morcos, S. Gopalakrishnan, and T. W. Nehl, "A Neuro-Fuzzy Approach to Automatic Diagnosis and Location of Stator Inter-Turn Faults in CSI-fed PM Brushless DC Motors," *IEEE Trans. Energy Convers.*, vol. 20, no. 2, pp. 253-259, Jun. 2005.

[7] Y. Lee and T. Habetler, "An On-line Stator Turn Fault Detection Method for Interior PM Synchronous Motor Drives," in *Proc. 22nd Annu. IEEE APEC*, Feb. 25–Mar. 1, 2007, pp. 825-831.

[8] J. Arellano-Padilla, M. Sumner, and C. Gerada, "On-line Detection of Stator Winding Short-Circuit Faults in a PM Machine Using HF Signal Injection," in *Proc. 18th ICEM*, Sep. 6–9, 2008, pp. 1-8.

[9] J. Chai, J. Wang, K. Atallah, and D. Howe, "Performance Comparison and Winding Fault Detection of Duplex 2-Phase and 3-Phase Fault-Tolerant Permanent Magnet Brushless Machines," in *Conf. Rec. 42nd IEEE IAS Annu. Meeting*, Sep. 23–27, 2007, pp. 566-572.

[10] Z. Sun, J. Wang, D. Howe, and G. Jewell, "Analytical Prediction of the Short-Circuit Current in Fault-Tolerant Permanent-Magnet Machines," *IEEE Trans. Ind. Electron.*, vol. 55, no. 12, pp. 4210-4217, Dec. 2008.

[11] Q. Chen, G. Liu, W. Gong, and W. Zhao, "A New Fault-Tolerant Permanent-Magnet Motor for Electric Vehicle Applications," *IEEE Trans. Magn.*, vol. 47, no. 10, pp. 4183-4186, 2011.

[12] K. H. Kim, D. U. Choi, B. G. Gu, and I. S. Jung, "Fault Model and Performance Evaluation of an Inverter-fed Permanent Magnet Synchronous Motor under Winding Shorted Turn and Inverter Switch Open," *IET Electr. Power Appl.*, vol. 4, no. 4, pp. 214-225, Apr. 2010.

[13] L. Romeral, J. C. Urresty, J. R. Riba Ruiz, and A. Garcia Espinosa, "Modeling of Surface-Mounted Permanent Magnet Synchronous Motors with Stator Winding Inter-Turn Faults," *IEEE Trans. Ind. Electron.*, vol. 58,no. 5, pp. 1576-1585, May 2011.

[14] B. Akin, S. Choi, U. Orguner, and H. Toliyat, "A simple Real-time Fault Signature Monitoring Tool for Motor Drive Embedded Fault Diagnosis Systems," *IEEE Trans. Ind. Electron.*, vol. 58, no. 5, pp. 1990-2001, May 2011.

Guohai Liu received the B.Sc. from Jiangsu University, China, in 1985, and the M.Sc and Ph.D. degrees from Southeast University, China, in 1988 and 2002, respectively, in electrical engineering and control engineering. Since 1988, he has been with Jiangsu University, where he is currently a Professor, the Dean of the School of Electrical Information Engineering. His teaching and research interests include electrical machines, motor drives for electric vehicles and intelligent control. He has authored or coauthored over 150 technical papers and 4 textbooks, and holds 15 patents in these areas.

Wei Tang received the B.Sc. degree in electrical engineering from Jiangsu University, Zhenjiang, China, in 2010. He is currently working toward the M.Sc. degree in electrical engineering at Jiangsu University, Zhenjiang, China. His research interests include condition monitoring and fault diagnosis of permanent magnet motor.

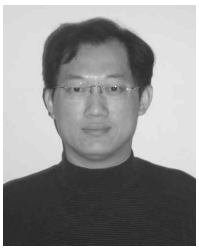

Wenxiang Zhao received the B.Sc. and M.Sc. degrees in electrical engineering from Jiangsu University, Zhenjiang, China, in 1999 and 2003, respectively, and the Ph.D. degree in electrical engineering at Southeast University, Nanjing, China, in 2010. Since 2003, he has been with Jiangsu University, where he is currently an Associate Professor in the School of Electrical Information Engineering. His areas of interest include electric machine design, linear motor and intelligent control.